A shallow-flow model for the propagation of tsunamis over mobile boundaries

D. Conde, R. Canelas,
Instituto Superior Técnico, Civil Engineering Department, Lisbon

J. Murillo
University of Zarazoza

C. Sousa Oliveira & R.M.L. Ferreira
Instituto Superior Técnico, Civil Engineering Department, Lisbon

SUMMARY:
A recent revision of the catalogue of tsunamis in Portugal has shown that Tagus estuary has been affected by catastrophic tsunamis numerous times over the past two millennia. This justifies the modelling efforts aimed at quantifying potential inundation areas for present-day altimetry and bathymetry of Tagus estuary. The purpose of this work is to present a 2DH mathematical model applicable to discontinuous shallow flows over complex geometries such as tsunami propagation overland. The conceptual model and the discretization scheme are presented and validation tests are described. The propagation of a tsunami with the magnitude of that of 1755 is simulated for the bathymetric and altimetry conditions of present day Tagus estuary. The study shows that some locations of Tagus estuary are vulnerable to tsunami impacts, as they may register 1 to 2 m flow depths and velocities of 5 ms^{-1}.

Keywords: Mathematical modelling, tsunami, Tagus estuary

1. INTRODUCTION

Tsunamis are waveforms mostly originated by the vertical displacement of the seafloor, as a consequence of an earthquake. They propagate in the ocean as deep waves carrying a large amount of kinetic energy. Yet, in deep waters, they exhibit low amplitude, relatively to the mean local sea level, which makes them difficult to observe directly. As they travel up the continental slope, the wavelength typically reduces and the amplitude increases. Approaching shore, the waves may break and form bores that propagate overland (Yeh, 1991). At this stage the tsunami becomes particularly destructive as its large amount of momentum is imparted to the obstacles it encounters. It incorporates debris, either natural sediment eroded from the bottom boundary or remains of human built environment, propagating as a granular-fluid flow. Bed morphology may be severely affected as the tsunami propagates inland and also as it recedes back to the ocean, as shown in the recent 2004 and 2011 occurrences in Sumatra and Japan, respectively.

A recent revision of the catalogue of tsunamis in Portugal has shown that Tagus estuary has been affected by catastrophic tsunamis numerous times over the past two millennia (Baptista et al. 2009). This justifies the modelling efforts aimed at quantifying potential inundation areas for present-day altimetry and bathymetry of Tagus estuary. Such modelling efforts have been undertaken recently (Baptista et al. 2011) but improvements can be achieved both in conceptual model and discretization techniques.

The purpose of this work is to present a 2DH mathematical model applicable to discontinuous flows over complex geometries such as tsunami propagation overland. The model is based on conservation equations of mass and momentum of water and granular material, derived within the shallow flow hypothesis, constituting a hyperbolic system of conservation laws. It features non-equilibrium sediment transport, conceived as an imbalance between capacity and actual bedload discharge. Flow friction, capacity bedload discharge and the characteristic length describing return-to-capacity require

closure equations (details in Ferreira et al. 2009). This conceptual approach allows for the description of a tsunami once it has incorporated debris and interacts with bed morphology.

The numerical model is developed within the Finite-Volume framework and based on the discretization technique presented by Murillo & García-Navarro (2010), allowing for fully conservative solutions to initial value problems (IVPs). The discretization of the non-homogeneous terms related to bed slope leads to a well-balanced scheme (Toro, 2001, Vázquez-Cendón, 1999). A robust wetting-drying algorithm, entropy conditions to prevent non-physical shocks and a revised Courant condition (Murillo & Garcia-Navarro, 2010) complete the numerical model. The numerical approach enables body-fitting unstructured meshes. This allows for optimization of computational effort, since the domain can be discretized with large cells, where flow gradients are small, and with small cells in the vicinity of flow obstacles (such as buildings) and, in general, where flow gradients are expected to be large. This model will herein be designated by STAV2D.

The conceptual model, fundamental of the discretization approach, the validation tests and the simulation of the 1755 tsunami in present-day Tagus estuary are shown in the following sections.

2. CONCEPTUAL MODEL

2.1. Conservation equations

Idealising the interaction between the bed and the flow as net normal flux of fluid and sediment, the application of the Reynolds Transport Theorem (RTT) to the total mass, momentum in both directions, sediment mass in the flow column and sediment mass in the bed, yields

$$\partial_t h + \partial_x (hu) + \partial_y (hv) = -\partial_t Z_b \tag{2.1}$$

$$\partial_t (uh) + \partial_x \left(u^2 h + \tfrac{1}{2} g h^2\right) + \partial_y (uvh) = -gh\partial_x Z_b - \frac{1}{\rho_m}\partial_x hT_{xx} - \frac{1}{\rho_m}\partial_y hT_{xy} - \frac{\tau_{b,x}}{\rho_m} \tag{2.2}$$

$$\partial_t (vh) + \partial_x (uvh) + \partial_y \left(v^2 h + \tfrac{1}{2} g h^2\right) = -gh\partial_y Z_b - \frac{1}{\rho_m}\partial_y hT_{yy} - \frac{1}{\rho_m}\partial_x hT_{yx} - \frac{\tau_{b,y}}{\rho_m} \tag{2.3}$$

$$\partial_t (C_m h) + \partial_x (C_m hu) + \partial_y (C_m hv) = -(1-p)\partial_t Z_b \tag{2.4}$$

and

$$(1-p)\partial_t Z_b = (q_s - q_s^*)/\Lambda \tag{2.5}$$

where x, y are the space coordinates, t is the time coordinate, h is the fluid height, u and v are the depth-averaged velocities in the x and y directions, respectively, Z_b is the bed elevation, ρ_m and C_m represent the depth-averaged density and concentration of the mixture, respectively, T_{ij} are the depth-averaged turbulent stresses, τ_b represents the friction exerted by the bed on the fluid, q_s is the sediment discharge, q_s^* is its capacity value and Λ is an adaptation length. The inertia of the granular material and the added pressure are neglected in the momentum equations (2.2) and (2.3).

2.2. Closure equations

The bed shear stress, τ_b, is such that

$$|\tau_b| = \rho C_f |u|^2 \tag{2.6}$$

where ρ is the water density. The friction coefficient, C_f, can be expressed by the Manning-Strickler formula or, for stratified flows, by the formula proposed by Ferreira et al. (2009). The turbulent stress tensor is $T_{ij} = \rho \nu_T \left(\partial_{x_j} u_i + \partial_{x_i} u_j \right)$ where the eddy viscosity, ν_T, is expressed by a simplified, zero-equation $k - \epsilon$ model (Pope, 2000).

Several bedload formulas can be used in STAV2D to describe capacity bedload transport, among them the well-known Meyer-Peter & Müller, 1947, and Bagnold, 1966, formulas (see Yalin, 1977). A specific formula for stratified flows (sheet flow) and debris flow is also incorporated. The bedload discharge is defined as $q_s^* = C_c^* |\mathbf{u}_c| h_c$ where C_c^* and $\mathbf{u}_c$ are the layer-averaged capacity concentration and velocity, respectively, in the contact load layer. Assuming that the thickness of the contact load layer, h_c, is related to the flux of kinetic energy associated to the fluctuating motion of transported grains (Ferreira et al., 2009), one has

$$h_c / d_s = m_1 + m_2 \theta \tag{2.8}$$

where d_s is the characteristic particle diameter, m_1 and m_2 are parameters that should depend on the mechanical properties of the sediment particles, on its diameter and density and on the viscosity of the fluid (see Ferreira, 2005, pp. 283-285), $\theta = C_f |\mathbf{u}^2| / \left(g(s-1) d_s \right)$ and s is the particles specific gravity. The layer velocity $\mathbf{u}_c$ can be considered can be taken as

$$\mathbf{u}_c = \mathbf{u} \left(h_c / h \right)^{1/6} \tag{2.9}$$

The capacity concentration, C_c^*, was also derived by Ferreira et al. (2009) assuming equilibrium of the frictional sub-layer. One obtains

$$C_c^* = \theta / \left(\tan(\varphi_b)(m_1 + m_2 \theta) \right) \tag{2.10}$$

where $\tan(\varphi_b)$ is the dynamic friction angle of the granular material (the ratio between normal and shear granular stresses, Bagnold, 1954). The adaptation length is susceptible to be chosen by the user. In this text, a formula proposed by Canelas et al. (2012) is employed.

3. DISCRETIZATION TECHNIQUE

The hyperbolic, non-homogeneous, first order, quasi-linear system of conservation laws, equations (2.1) to (2.4), can be written in compact notation:

$$\partial_t \mathbf{U}(\mathbf{V}) + \partial_x \mathbf{F}(\mathbf{U}) + \partial_y \mathbf{G}(\mathbf{U}) = \mathbf{H}(\mathbf{U}) \tag{3.1}$$

with

$$\mathbf{V} = \begin{bmatrix} h \\ u \\ v \\ C_m \end{bmatrix}; \ \mathbf{U} = \begin{bmatrix} h \\ uh \\ vh \\ C_m h \end{bmatrix}; \ \mathbf{F} = \begin{bmatrix} uh \\ u^2 h + \frac{1}{2} gh^2 \\ uvh \\ C_m hu \end{bmatrix}; \ \mathbf{G} = \begin{bmatrix} vh \\ vuh \\ v^2 h + \frac{1}{2} gh^2 \\ C_m hv \end{bmatrix} \text{ and } \mathbf{H} = \begin{bmatrix} -\partial_t Z_b \\ -gh\partial_x Z_b - \tau_x / \rho \\ -gh\partial_y Z_b - \tau_y / \rho \\ -\partial_t Z_b (1 - p) \end{bmatrix},$$

where $\mathbf{V}$ and $\mathbf{U}$ are the vectors of primitive and conservative dependant variables, respectively, $\mathbf{F}$ and $\mathbf{G}$ are the flux vectors, in x and y direction, $\mathbf{H}$ is the vector of source terms and

$\tau_i = \tau_{b,i} + \partial_{x_i} hT_{ii} + \partial_{x_j} hT_{ij}$. Employing Godunov's finite-volume approach (Leveque, 2002), discretization, the system (3.1) is integrated in a cell i. The following explicit flux-based finite-volume scheme is obtained

$$\mathbf{U}_i^{n+1} = \mathbf{U}_i^n - \frac{\Delta t}{A_i} \sum_{k=1}^{3} L_k \sum_{m=1}^{4} \left(\tilde{\lambda}^{(m)} \alpha^{(m)} - \beta^{(m)} \right)_{ik}^{-} \tilde{\mathbf{e}}_{ik}^{(m)} + \Delta t \left(\mathbf{R}_i^{n+1} \right) \tag{3.2}$$

where Δt is the time step, obeying a Courant condition ($CFL \leq 1$), A_i is the cell area, L_k is the edge length, $\tilde{\mathbf{e}}^{(m)}$ is the m-th approximate eigenvector, $\tilde{\lambda}^{(m)}$ is the m-th approximate eigenvalue (Roe, 1981), $\alpha^{(m)}$ and $\beta^{(m)}$ are the wave strengths associated to conservative and non-conservative ($gh\partial_{x_i} Z_b$) fluxes, respectively, and $\mathbf{R}_i^{n+1} = \left(\left[\partial_t Z_b - \tau_x / \rho_m - \tau_y / \rho_m \quad \partial_t Z_b (1-p) \right]^T \right)_i^{n+1}$ is the parcel of the source terms not susceptible to be treated as a non-conservative fluxes. Terms $gh\partial_{x_i} Z_b$ are not physical fluxes; they are treated as so to obtain a well-balanced numerical scheme (Vásquez-Cendón, 1999). Only the negative part of the eigenvalues $\tilde{\lambda}_{ik}^{(m)}$ and of $\beta_{ik}^{(m)}$ coefficients are used, ensuring that only incoming fluxes are used in the update of the conserved variables. The approximate eigenvalues and eigenvectors and the wave strengths are calculated as in Murillo et al. (2010). Further details on the numerical scheme can be found in Canelas et al. (2012) and Murillo et al. (2010), namely in what concerns wetting/drying algorithms, entropy conditions, Courant condition and discretization of turbulent stresses.
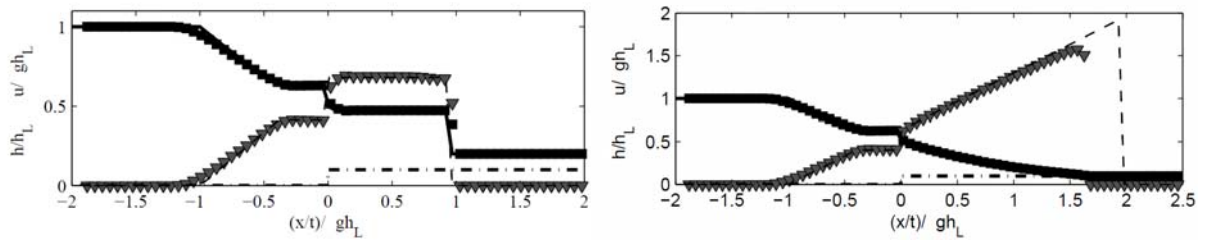

4. VALIDATION

4.1. Stoker solution for dam-break flows over fixed flat smooth beds

The dam-break problem over fixed flat smooth beds is an IVP that admits theoretical solutions (Stoker 1957). The fundamental non-dimensional parameters that describe the initial conditions are

$$\alpha \equiv \left(h_R + \left| \min(0, Z_{b_l}) \right| \right) \Big/ \left(h_L + \max(0, Z_{b_l}) \right); \qquad \delta \equiv Z_{b_l} \Big/ \left(h_L + \max(0, z_{b_l}) \right) \tag{4.1}$$

where h_R and h_L are the initial fluid depths of the right and left states, respectively, and Z_{b_l} is the bed elevation on the left side considering the right side as the reference horizontal plane. The solution, according to Lax theorem (Leveque, 2002), features two waves (shocks or rarefaction waves), separated by a constant state. When $h_L = 10.0$ m, $h_R = 1$ m, $\alpha = 0.2$ and $\delta = -0.1$, the solution features a downstream-progressing shock, an upstream-progressing rarefaction wave and a discontinuity at the bed jump (Alcrudo & Benkhaldoum, 2001). The problem is 1D but the discretization is 2DH with triangular cells with an average side of 0.65 m for a channel 10.0 m wide. The numerical results, obtained with $CFL = 0.8$, are shown in Figure 4.1(left), along with the theoretical solution.

The numerical solution reproduces correctly the analytical weak solution. The energy dissipation induced by the bottom source terms is correctly evaluated and the shock speeds are correctly described. The effects of the numerical dissipation are visible (as profile smoothing) in the interface between the left state and the expansion wave and between the constant intermediate states. When $h_L = 10.0$ m, $\alpha = 0.1$ and $\delta = -0.1$, the solution features a downstream-progressing expansion wave, an upstream-progressing rarefaction wave and a discontinuity at the bed jump. The computed solution correctly follows the structure of the theoretical solution. However, the velocity at the wave front is underestimated because of the flux reduction imposed by the wetting-drying algorithm.

Figure 4.1. Stoker solution with corresponding numerical solution. Left: $\alpha = 0.2$ and $\delta = -0.1$. Right: $h_L = 10.0$ m, $h_R = 1$ m, $\alpha = 0.1$ and $\delta = -0.1$

The validation tests show that discontinuous solutions are correctly reproduced, although the scheme introduces diffusion and wave attenuation, especially for coarse grids.

4.2. Laboratory benchmark test

Laboratory results, gathered within the framework of the NSF/PIRE-funded project "Modelling of Flood Hazards and Geomorphic Impacts of Levee Breach and Dam Failure", at the experimental facilities of the Université catholique de Louvain (Soares Frazão et al. 2012), were used to validate the model in a dam-break test over mobile bed. The experimental facilities consist of a 3.6 m wide and 36 m long flume fully instrumented with flow and bed elevation ultrasonic probes and flow visualisation. The dam is represented by two impervious blocks and a 1.0 m wide gate, located between the blocks. The bed was a 85 mm thick layer of sand with $d_{50} = 1.61$ mm and $s = 2.56$. The test employed for validation featured $h_L = 0.47$ m and $h_R = 0.0$ m. The available data consists in measurements of the time-evolution of the water elevation at 8 gauging points (see Canelas et al. 2012) and longitudinal final bed profiles, measured in a continuous way from $x = 0.5$ m to $x = 8$ m with a Δy spacing of 0.05 m. The combination of all profiles allowed for the reconstruction of the three-dimensional final bed topography.

The results are shown in Figures 4.2 and 4.3. Figure 4.2 shows the final bed topography (left) and respective simulation, employing Bagnold's as transport capacity formula. It is observed that the model reproduces correctly the main traits of the deposition pattern.
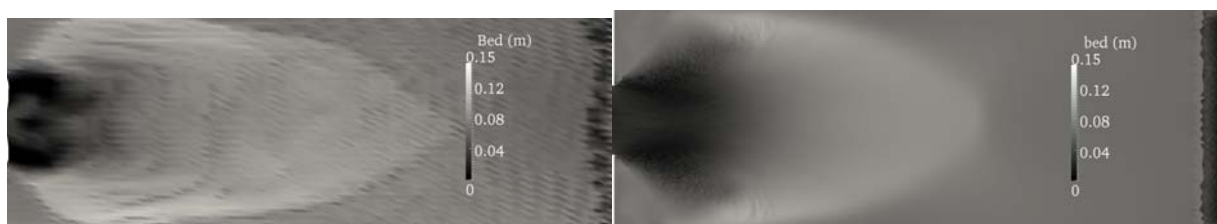
Figure 4.2. Final bed topography (60 s) of benchmark test. Left: measurements. Right: numerical simulation with Bagnold capacity formula, flow resistance and adaptation length in accordance to Canelas et al. (2012).

Figure 4.3 shows longitudinal bed profiles taken at three different lateral positions with superimposed numerical results, obtained with three different bedload capacity formulas. The comparison shows that the solution is somewhat sensitive to the particular choice of formula describing bedlaod capacity.

The main features of the observed bed profiles are captured by the numerical solutions: strong erosion near the gate and an aggradation wave spanning from 3 to 6 m downstream the gate. The lateral extension of the scour hole, related to the magnitude of the recirculation zone, is the only feature whose modelling needs improvement. The main issue concerns the orientation of the sediment movement relatively to the fluid flow (not necessarily aligned), for which the present state-of-the-art is very limited.
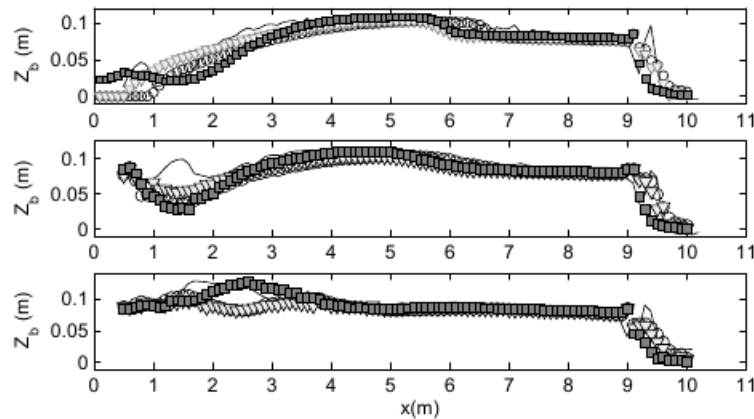
Figure 4.3. Longitudinal bed profiles for $y = 0.20$, $y = 0.70$ and $y = 1.45$ m. Measured (——) and simulated profiles with capacity transport formulas of Ferreira (2009) (○), Meyer-Peter & Müller (▽) and Bagnold (◼). Adaptation length and friction factor in accordance with Canelas et al. (2012).

The validations tests demonstrate that the model is robust and can simulate discontinuous flows over complex mobile beds. Its main shortcomings reflect general poor knowledge on phenomenological issues related to the interaction between flow and bed morphology.

5. APLICATION: A 1755 TSUNAMI IN TODAY'S TAGUS ESTUARY

STAV2D was employed to simulate a tsunami similar to that occurred in the 1st of November of 1755, in present-day Tagus estuary. Two scenarios were considered: low and high tide, defined as -2 m and +2m, respectively, relatively to reference zero.

The digital elevation model including Tagus bathimetry, with a 10 m resolution, was obtained from Luís (2007). Bed is considered fixed in the waterfronts of Oeiras, Lisbon, Almada, Barreiro, Seixal and Montijo and mobile at all other locations.

Open boundary conditions, formalised in terms of Rankine-Hugoniot conditions, are prescribed at the Tagus valley and at the Atlantic reach (Figure 5.1). In the Tagus valley a constant discharge of 500 m^3s^{-1} (approximately the modular discharge) is introduced in the direction normal to the boundary. In the Atlantic boundary, it is introduced, at each cell in the boundary, a water elevation time series corresponding to the 1755, as calculated by Baptista et al. (2011). The main feature of these series is that they prescribe a water height, above tide level, of about 5 m at Bugio, in accordance to historical reports (Baptista et al. 2009). Figure 5.1 shows the first tsunami wave propagating over high tide, immediately after hitting Bugio. Water elevation, at Tagus mouth is about 7 m above reference zero, *i.e.* 5 m above high tide level.

Initial conditions comprise flow depths and velocities compatible with the discharge, at Tagus valley, of 500 m^3s^{-1} and tide level at the Atlantic boundary. The computational domain is composed of 125000 triangular cells, the smallest of which have 20 m long edges.

Simulation covers 2.7 hours after Bugio island is hit. The results are shown in Figures 5.2 to 5.5. Figure 5.2 shows the most noticeable morphological impacts in the Tagus estuary, occurring at Trafaria and Caparica atlantic coast. Widespread erosion, more than 1m deep, is registered at the end of the simulation period, mostly due to flow velocities higher than 5 ms^{-1}. The draw-down provokes also 1 m high deposits in some locations at Caparica beach and Trafaria. The sand banks at the Tagus mouth are displaced inwards by the incoming wave.
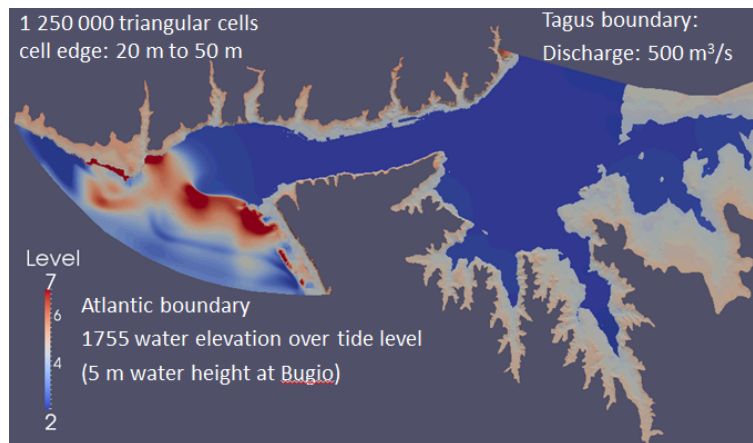
Figure 5.1. Simulation at high tide. Initial and boundary conditions.
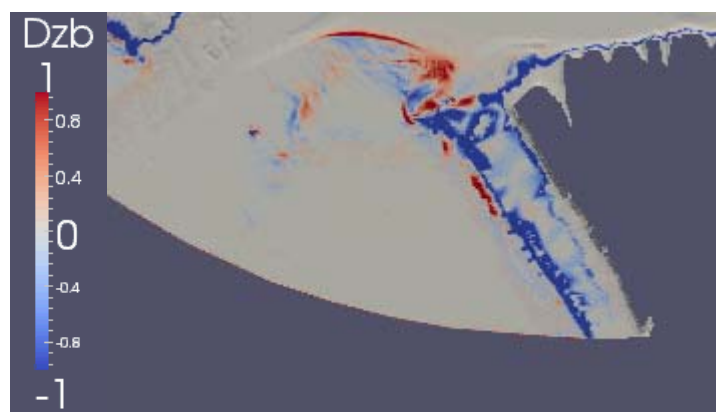
Figure 5.2. Main morphological impacts. Detail at Tagus mouth, Trafaria and Caparica beach.

The main impacts of the tsunami propagating over a low tide level are shown Figure 5.3, a detail of Lisbon Baixa. Inundation is limited to less than 1 m deep patches at Rocha do Conde de Óbidos, Cais do Sodré, Praça do Comércio and Sta. Apolónia. Velocities are low, less than 1 ms^{-1}. The extent of damage in this case would be limited, which is explained by the fact that landfills and protection works after 1755 left Lisbon waterfront about 5 m above low tide water elevation at the estuary if flow discharge at Tagus is low.

Figure 5.3. Low tide simulation. Water elevation (left) and velocity (right) at Baixa waterfront 20 min after hitting Bugio.

Figures 5.4 and 5.5 show the tsunami propagation on Lisbon waterfront at high tide. Figure 5.4 shows the results of the simulation at the Belém-Alcântara reach 9.5 to 14.5 min after the tsunami has hit

Bugio. The simulation indicates that, in this case, the tsunami could have a devastating impact. The run-up at Praça do Império and Jerónimos monastery could reach 500 m. At Alcântara, the largest run-up is about 550 m. Water heights (above local ground) can reach 2 m at Belém–Praça do Império and at Belém fortress. Flow velocities can reach 5 ms^{-1} at Alcântara harbour and at Belém.
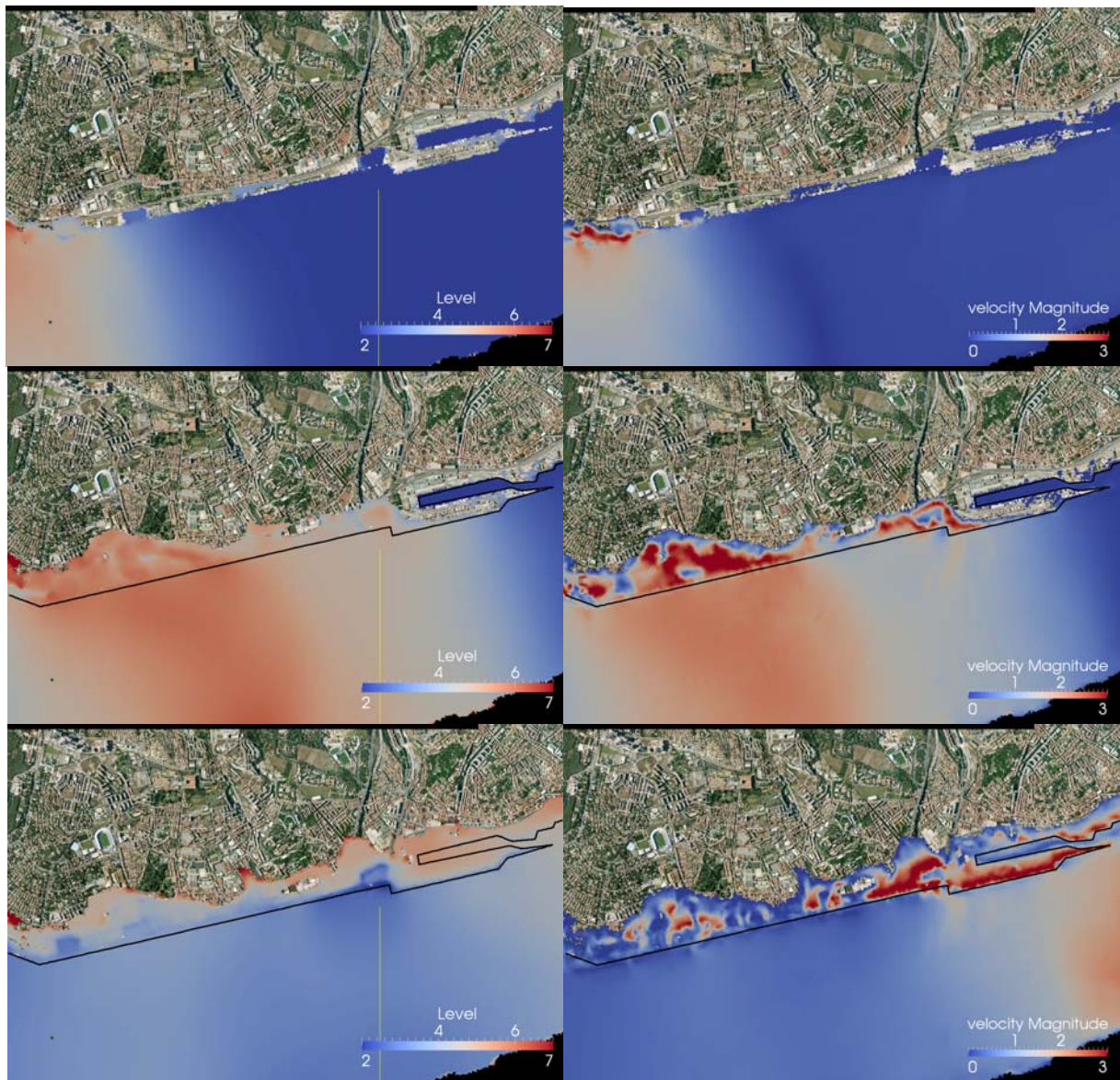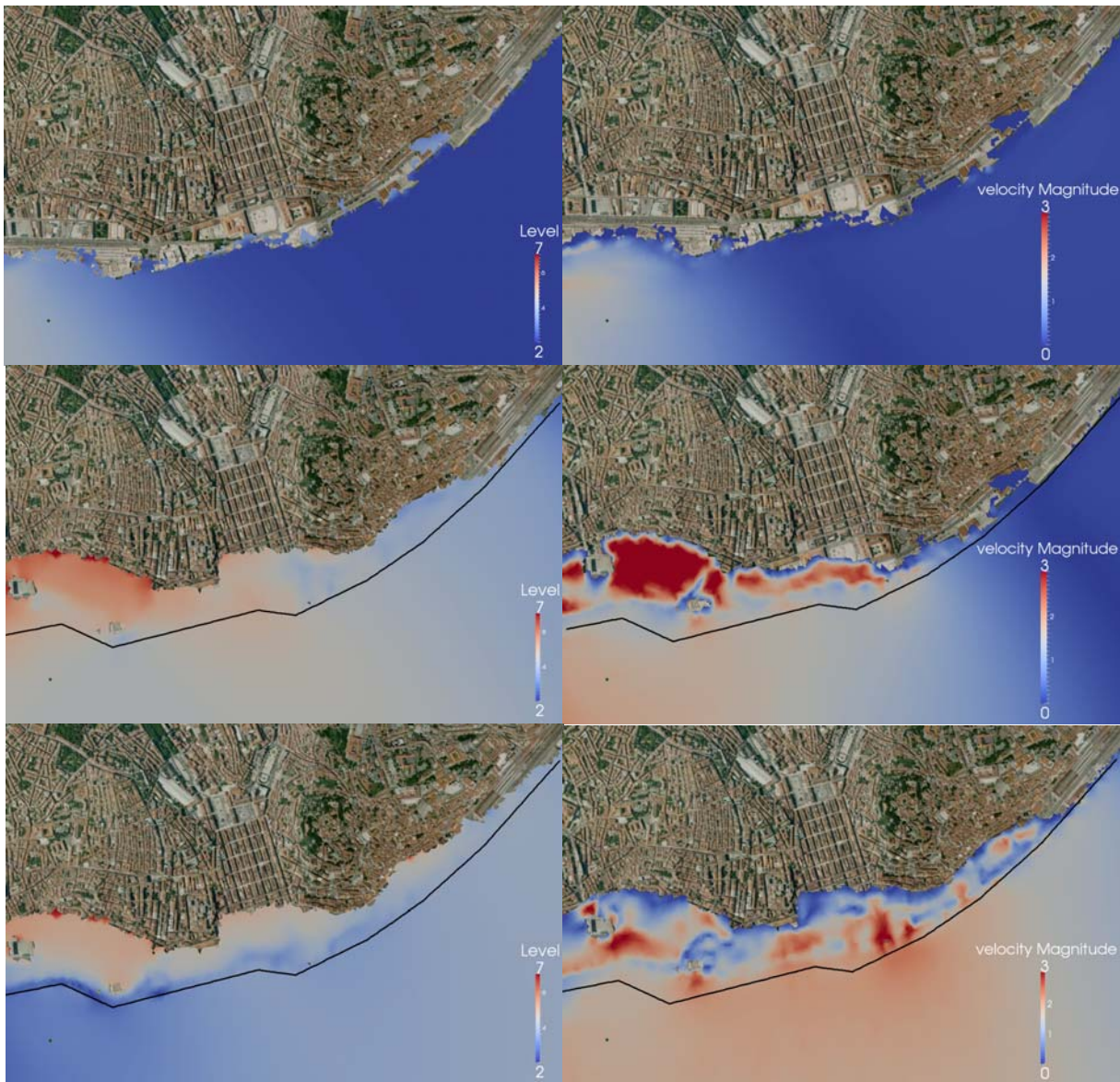

Figure 5.4. High tide simulation. Water elevation (left) and velocity (right) at Belém-Alcântara waterfront 9.5, 11 and 14.5 min after hitting Bugio.

Figure 5.5 shows the results of the simulation at high tide for the Baixa reach. Again, the simulation indicates that the tsunami would have major impacts on Lisbon waterfront. Praça do Comércio would be completely inundated and the wave would propagate inside Baixa meshwork of orthogonal streets. Run-up would be about 300 m at Baixa and 400 m at S. Paulo. Water depths could reach about 1.5 m at the shore line. Sta. Apolónia train station would also be reached by the incoming wave. Velocities of 3-4 ms^{-1} would be felt at Praça do Comércio at the beginning of the inundation at during run-out.

The results of the simulation are show larger run-up distances than those calculated by Baptista et al. (2006) and Baptista et al. (2011), which may be explained by the initial water elevation of the later study, coinciding with mean tide level and not high tide. Flow depths, however, are compatible with those calculated by Baptista et al. (2011) if the high tide level is added to the results of the latter study.

Velocities are not susceptible to be compared as they are not calculated in Baptista et al. (2011).

Figure 5.5. High tide simulation. Water elevation (left) and velocity (right) at Baixa waterfront 15.5, 16.5 and 19.5 min after hitting Bugio.

The detailed patterns of flow are beyond the scope of the present simulation effort since the employed DEM does not have enough resolution to clearly distinguish streets and buildings. New simulations will be performed in sensitive areas such as Belém, Alcântara and Baixa with actual street geometry.

6. CONCLUSION

The propagation of a tsunami with the magnitude of that of 1755 was simulated for the bathymetric and altimetry conditions of present day Tagus estuary. The simulated water elevations featured a maximum wave height of 5 m above tide level at Bugio. The simulation tool was STAV2D, a mathematical model of numerical solution applicable to shallow flows that carry sediment load, interact with the bottom and may develop bores or other type of discontinuities. The model has been validated with theoretical solutions and laboratory measurements.

The analysis of results of the simulation reveals that morphological impacts are relevant in Trafaria

and Caparica atlantic beach, with 1 m deep generalized erosion of the shoreline and deposits of more than 1 m at several locations. Morphological impacts are especially important at high tide.

At the Lisbon water front, the simulations show that the combination of high tide and tsunami can lead to major devastation in sensitive areas such as Belém, Alcântara, S. Paulo or Baixa. At these locations run-up can reach 300 to 500 m. Flow depths may reach 1 to 2 m along the entire waterfront. The highest registered depths in the simulation occurred at Belém, in the vicinity of Belém fortress, an especially relevant touristic location. Velocities ranging between 4-5 ms^{-1} and 3-4 ms^{-1} would be felt at Praça do Comércio and Alcântara, both during run-up and just slightly lower at draw-down. High velocities associated with above-waist flow depths are especially worrisome as they are responsible for incorporation of debris and are associated to high casualties.

The study has shown that some locations of Tagus estuary are vulnerable to tsunami impacts. More detailed studies, featuring actual building geometry, are under way. These should provide data to design evacuation plans in case of a major tsunami.

REFERENCES

Alcrudo, F. & Benkhaldoun, F. (2001). Exact solutions to the riemann problem of the shallow water equations with a bottom step. *Computers and Fluids*, **30**, 643–671.

Bagnold, R. (1954). Experiments on a gravity-free dispersion of large solid spheres in a newtonian fluid under shear. In: *Proceedingsof the Royal Society of London*.

Baptista M.A.;Miranda, J.M.; Omira, R.; Antunes, C. (2011). Potential inundation of Lisbon downtown by a 1755-like tsunami. *Natural Hazards and Earth System Science*. (in press).

Baptista, M.A. & Miranda J.M. (2009). Revision of the Portuguese catalog of tsunamis. *Natural hazards and earth system sciences,* **9** (1): 25-42

Ferreira, R. M. L. (2005). *River Morphodynamics and Sediment Transport. Conceptual Model and Solutions*. Ph.D. thesis, Instituto Superior Técnico - Universidade Técnica de Lisboa, Lisboa.

Ferreira, R. M., Franca, M. J., Leal, J. G. & Cardoso, A. H. (2009). Mathematical modelling of shallow flows: Closure models drawn from grain-scale mechanics of sediment transport and flow hydrodynamics. *Canadian Journal of Civil Engineering*, **36**, 1604–1621.

IAHR-GDBFEB (Soares-Frazão, S. et al.) (2011). Dam-break flows over mobile beds: Experiments and benchmark tests for numerical models. *Journal of Hydraulic Research* (in press).

Leveque, R. (2002). *Finite Volume Methods for Hyperbolic Problems*. Cambridge University Press.

Luis, J.F. (2007). Mirone: A multi-purpose tool for exploring grid data. *Computers & Geosciences*, **33**, 31-41.

Murillo, J. & Garcia-Navarro, P. (2010). Weak solutions for partial differential equations with source terms: application to the shallow water equations. *J. Comp. Physics* **229**(11), 4327–4368.

Murillo, J.; García-Navarro, P., Brufau, P. & Burguete, J. (2010). 2d modelling of erosion/deposition processes with suspended load using. *Journal of Hydraulic Research,* **46**(1), 99–112.

Pope, S. B. (2000). *Turbulent Flows*. Cambridge University Press.

Roe, P. (1981). Approximate riemann solvers, parameter vectors and difference schemes. *J. Comp. Physics* **43**, 357–372.

Stoker, J.J. (1992). *Water waves. The mathematical with applications*. Willey Classic Library, (reprint of 1957 edition).

Toro, E. (2001). *Shock-Capturing Methods for Free Surface Shallow Flows*. Wiley, New York.

Vázquez-Cendón, M. (1999). Improved treatment of source terms in upwind schemes for the shallow water equations with irregular geometry. *J. Comp. Physics*, **148**,497.

Viana-Baptista, M. A.; Soares, P. M.. ; Miranda, J. M. & Luis, J. F. (2006). Tsunami Propagation Along Tagus Estuary (Lisbon, Portugal) Preliminary Results, *Science of Tsunami Hazards*, **24**(5), 329-.

Yalin, M. S. (1977). *Mechanics of Sediment Transport*. Oxford, UK: Pergamon Press, 2nd ed.

Yeh, H.H. (1991) Tsunami bore runup. *Natural Hazards* **4**(2-3), 209–220. DOI: 10.1007/BF00162788.